Journal of Hazardous Materials 221–222 (2012) 100–108

Contents lists available at SciVerse ScienceDirect

Journal of Hazardous Materials

journal homepage: www.elsevier.com/locate/jhazmat

Photocatalytic degradation of hexazinone and its determination in water via UPLC–MS/MS

Mei Mei [a], Zhenxia Du [a,*], Ruifen Xu [b], Yun Chen [a], Haojie Zhang [a], Shuping Qu [a]

[a] College of Science, Beijing University of Chemical Technology, Beijing, China
[b] JiangSu KaoPuLe New Material Co., Ltd, Jiangsu, China

ARTICLE INFO

Article history:
Received 7 October 2011
Received in revised form 5 April 2012
Accepted 6 April 2012
Available online 17 April 2012

Keywords:
Photocatalytic degradation
Mixed-phase crystal nano-TiO_2
UPLC–MS/MS
Hexazinone

ABSTRACT

Degradation of hexazinone has been investigated by means of photocatalysis of mixed-phase crystal nano-TiO_2. Influences of adsorption, amount of nano-TiO_2, pH and irradiation time on the photocatalytic process are studied. Results show that hexazinone is totally degraded within 40 min of irradiation under pH neutral conditions. This compares favorably with Degussa P25 TiO_2 when conducted under the same experimental conditions. Preliminary photocatalytic kinetic information for hexazinone degradation is proposed. First order kinetics is obtained for the adsorption and photocatalytic degradation reactions, which fit the Langmuir–Hinshelwood model. A rapid, sensitive and accurate UPLC–MS/MS technique is developed and utilized to determine the level of hexazinone in water in support of the degradation kinetics study. The results indicate a limit of detection (LOD) at 0.05 μg/l and the recoveries between 90.2 and 98.5% with relative standard deviations (RSD) lower than 12%. A LC–MS/MS technique is used to trace the degradation process. Complete degradation is achieved into final products including nontoxic water, carbon dioxide and urea. A probable pathway for the total photocatalytic degradation of hexazinone is proposed.

1. Introduction

It is increasingly important nowadays to develop effective method for monitoring and remediation on environmental pollutants in water. Hexazinone [3-cyclohexyl-6-(dimethylamino)-1-methyl-1,3,5-triazine-2,4 (1H, 3H)-dione] is a broad-spectrum herbicide. It may be absorbed through either the roots or the leaves and acts as an inhibitor to photosynthesis [1]. It has been registered by the Environmental Protection Agency (EPA) for use on railroad, highway, industrial plant sites, woodland management areas, and in agriculture on alfalfa, pasture, range grasses, pineapples, sugarcane and blueberries [2].

Hexazinone is highly soluble in water (33 g/l at 25 °C) and mobile in soil. These characteristics lead to great potential for leaching into ground water and for overland runoff into surface water [3]. Hexazinone is considered to be among the most likely pesticides to contaminate ground water. There is evidence that field applications of hexazinone have resulted in surface water contamination, which raises great concerns about its safety to wildlife and human health [1,4]. Therefore, determination and degradation of hexazinone in water is in great need.

Previous study on this herbicide mainly focused on residual determination methods, such as HPLC [5], LC–MS and GC–MS [6], and CE [4]. Among these methods, UPLC–MS/MS has many advantages such as high separation ability, high sensitivity, wide application scope and high specificity.

Hexazinone is regarded to be unsusceptible to hydrolysis [7] and photolysis [8], so it can persist in the aquatic systems. To degrade the herbicide, anaerobic biodegradation [9] and electro-reduction [10] have been reported. However, there are few reports for photocatalysis degradation of hexazinone. Photocatalysis, as an advanced oxidation process (AOP), has received significant attention in water or wastewater treatment due to its powerful oxidative capability, low cost, nontoxicity and chemical stability [11–13]. This technique is based on the use of UV-irradiated semiconductors (generally titania under the form of rutile or anatase). When TiO_2 is irradiated with photons whose energy equals or exceeds its band gap energy (EG = 3.0 or 3.2 eV with $\lambda < 390$ nm), electron–hole pairs are created. In aqueous system, the holes react with H_2O or OH^- adsorbed at the surface of the semiconductor to produce $OH^\bullet$ radicals which are the most oxidizing species in this process. On the other hand, electrons are trapped at surface sites and removed by reactions with adsorbed molecular O_2 to form superoxide anion radical $O_2^{\bullet -}$. Several modifications have been attempted to increase the photoactivity of TiO_2. Significant improvement has been achieved with the use of TiO_2 nanoparticles [14–16]. In our work, the mixed-phase crystal

* Corresponding author. Tel.: +86 10 64433909; fax: +86 10 64433909.
E-mail address: duzx@mail.buct.edu.cn (Z. Du).

0304-3894/$ – see front matter © 2012 Elsevier B.V. All rights reserved.
http://dx.doi.org/10.1016/j.jhazmat.2012.04.018

nano-TiO_2 has been studied as a way of increasing the TiO_2 photoactivity which compares favorably with Degussa P25. This can be explained by the appropriate mixed-phase microstructure allowing electron transfer process and by the characteristics of nano particles.

The main objective of this research is to study the efficient and nontoxic degradation of hexazinone with use of photocatalytic techniques. The kinetics, influencing parameters and pathway of degradation are reported. An UPLC–MS/MS methodology is developed and used to support this study.

Several new approach and results are reported in our study. Specifically:

- Use of photocatalytic degradation on hexazinone is investigated
- Small and nontoxic photocatalytic degradation by-products are identified
- Pathway for complete degradation is proposed

Photocatalytic degradation and UPLC–MS/MS methodology have significant potential for the routine remediation and monitoring of dissolved pollutants in water and may have great potential for a wide range of practical applications.

2. Experimental

2.1. Materials and reagents

Hexazinone [3-cyclohexyl-6-(dimethylamino)-1-methyl-1,3,5-triazine-2,4 (1H, 3H)-dione] (98% purity) was provided by China Standard Material Research Center. HPLC-grade organic solvents were purchased from Fisher Scientific (Loughborough, UK). Ultra pure water was obtained from a Milli-Q (Millipore, Milford, MA, USA) water purification system. The mixed-phase crystal nano-TiO_2 photocatalyst was provided by JiangSu KaoPuLe New Material Co., Ltd.

2.2. Characterization techniques

The phase and crystal structure of the product were determined by X-ray diffraction (XRD), which were recorded with a Philips X'Pert PRO MPD X-ray diffractometer using Cu-Kα radiation (λ = 1.54178 Å). Diffraction patterns of both anatase and rutile phase were compared with reference to JCPDS (21-1272, 21-1276) powder diffraction files. From the line broadening of the corresponding X-ray diffraction peaks and using the Scherrer's formula, the crystallite size has been estimated by [17,18]:

$$L = \frac{K\lambda}{\beta \cos\theta}$$

where L is the average crystallite size in nm, λ is the wavelength of the X-ray radiation (0.154056 nm for copper lamp), K is a constant usually taken as 0.9, β is the line width at half-maximum height in radians, and θ is the diffracting angles. The % anatase was calculated by the following non-linear equation [19,20]:

$$\%A = \frac{100}{(1 + 1.265 I_R/I_A)}$$

where $\%A$ = anatase content in percent, I_A = peak intensity of the peak at $2\theta = 25^\circ$, R = peak intensity of the peak at $2\theta = 28^\circ$.

The TEM micrographs were performed on a Jeol apparatus (JEM-3010). Particle size distribution test was performed by NanoZS Nano granularity cryoscope (MaErWen, British). The band gap energies of titanium dioxide samples were determined using UV–vis spectrophotometer equipped with an integrating sphere accessory (Shimadzu UV-3010). The spectra were recorded in diffused reflectance mode with $BaSO_4$ as a reference. The band gap energies (E_g) of the catalyst were calculated by the Planck's equation:

$$E_g = \frac{hc}{\lambda} = 1240\lambda$$

where E_g is the band gap energy (eV), h is the Planck's constant, c is the light velocity (m/s), and λ is the wavelength (nm).

2.3. Photocatalytic experiments

A series of photocatalytic experiments were performed to investigate the degradation behavior of hexazinone. Some important parameters including adsorption, amount of catalyst, pH and irradiation time were estimated.

Before the irradiation experiments, preliminary adsorption experiments were carried out in the dark to study the isotherm adsorption of the hexazinone on TiO_2 surface. The herbicide aqueous suspensions were shaken in the dark for 30 min (at 35 °C, 180 rpm), and 100 μl of the samples were collected regularly.

The irradiation reactions were carried out with a UV light in a dark box where a glass vessel with an optical window of 12.5 cm^2 area was exposed to air. For all irradiation experiences, the TiO_2 suspensions were magnetically stirred in the glass vessel. The initial solution volume was 25 ml. The light source was a HPK 125 W Philips mercury lamp, cooled with water circulation. The lamp spectrum had a maximum emission at 365 nm. The radiant flux was measured using a radiometer (United Detector Technology Inc., Model 21A power meter). It has been detected that the number of photons potentially absorbable by TiO_2 in the irradiation cell could vary from 10 to 19 mW/cm^2.

2.4. Samples preparation

During the irradiation, 100 μl of the aqueous suspension was collected at regular times and filtered through 0.22 μm PES filters (MEMBRANA, Germany) to remove suspended particles. The filtering step is required to prevent plugging of the UPLC column. The standard solution and the aqueous suspension spiked with the standard solution before irradiation were also filtered through the PES filters. The results show the absence of hexazinone adsorption on these filters. This is consistent with the results reported in our previous work [21].

2.5. Analytical determinations

The determination step was performed with a Waters ACQUITY UPLC tandem Quattro Premier triple quadrupole mass spectrometer system (Waters, USA), equipped with an electrospray ionization (ESI) interface (Z-spray). The tandem mass spectrometer was operated in a positive electrospray ionization mode (ESI^+).

The LC–MS/MS identification of photocatalytic by-products was performed with the following source parameters: capillary voltage 3.0 kV; sample cone voltage 25 V; collision energy (CE) 15 eV; source temperature 100 °C; and desolvation gas temperature 350 °C. The flow rates for desolvation gas and cone gas (N_2) were set at 600 and 50 l/h, respectively.

For increased sensitivity and selectivity, data acquisition was performed in multiple reaction monitoring (MRM) mode. For instrument control, data acquisition and processing MassLynx and QuanLynx software 4.1 was used.

The MRM parameters are shown in Table 1. The UPLC measurement was performed with a BEH C18 (50 mm × 2.1 mm I.D., 1.7 μm) column. The gradient program was as following: from 40% A (methanol) and 60% B (ultra pure water) to 98% A in 2.5 min, then a linear ramp to 40% A in 0.5 min. The system mobile phase flow rate

Table 1
MRM parameters for hexazinone.

Compound	Retention time (min)	Precursor ion	Daughter ion	Collision energy (eV)	Cone voltage (V)
Hexazinone	1.83	253.0	253.0 > 170.4[a] 253.0 > 70.2	18 20	28 28

[a] Quantitative ion.

was 0.25 ml/min, the injection volume was 5 μl, and the column temperature was maintained at 30 °C (ambient).

3. Results and discussion

3.1. Determination of hexazinone in water samples

Fig. 1 shows the UPLC–MS/MS spectra for hexazinone and water. The determination of hexazinone was done with doped MQ water samples. The UPLC–MS/MS method using the MRM mode for determination of hexazinone in water samples is rapid, sensitive, confirmed and specified.

Table 2 shows that the linear correlation coefficient of 0.9984 was obtained across a concentration range of 0.5–500 μg/l. Limits of detection (LOD) was 0.05 μg/l (S/N = 3), and the limits of quantification (LOQ) was 0.16 μg/l (S/N = 10). The method was validated with water samples spiked at two fortification levels (4 and 40 μg/l) and recoveries were estimated in the 90.2–98.5% range with relative standard deviations (RSD) lower than 12%. The results showed that the proposed method is sensitive, accurate and reproducible for determination of hexazinone in water samples. Furthermore, it is an effective analytical method for degradation studies of hexazinone in water.

3.2. Characterization of nano-TiO_2 catalyst

The photocatalytic activity of TiO_2 depends on various parameters, including crystalline form, impurity, particle size, and density of surface hydroxyl groups [22,23]. Fig. 2 shows the XRD spectra

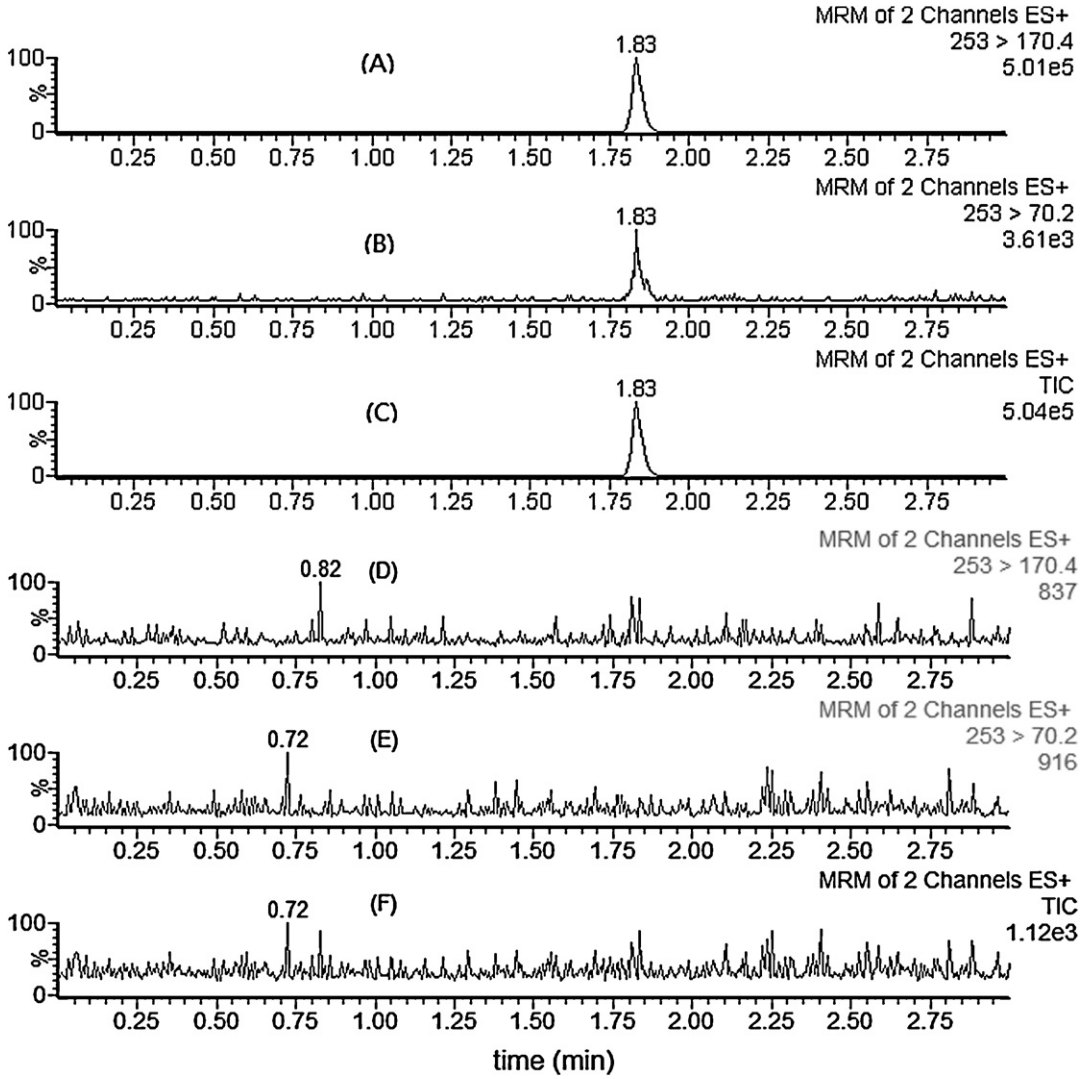

Fig. 1. Under the MRM mode, the UPLC–MS/MS spectra for hexazinone in water and blank water sample (A) and (D) the quantitative ion parents spectra, (B) and (E) the qualitative ion parents spectra, (C) and (F) the total ion scan spectra.

Table 2
Linear equations correlation coefficients LOD LOQ Recoveries and RSD.

Compound	Linear range (μg/l)	Linear equation	Correlation coefficients (r^2)	LOD (μg/l)	LOQ (μg/l)	Recovery (RSD) $n = 6$, %	
						Spiking 4 μg/l	Spiking 40 μg/l
Hexazinone	0.5–500	$y = 2139.22x - 427.944$	0.9984	0.05	0.16	90.2 (11.8)	98.5 (7.9)

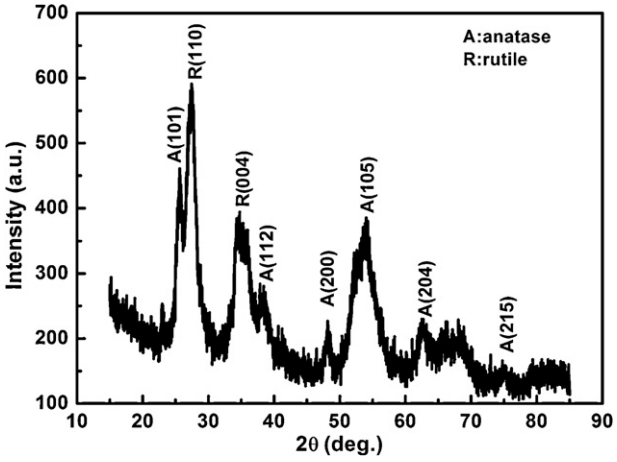

Fig. 2. XRD patterns of nano-TiO_2.

of the nano-TiO_2 catalyst. The nano-TiO_2 is a mixed-phase crystal of the anatase and rutile (1:1). Usually, TiO_2 is used as a photocatalyst in two crystal forms: rutile and anatase. Interestingly, the photoactivity of TiO_2 consisting of variable anatase–rutile ratio and appropriate microstructure characteristics and morphology exceeds that of pure anatase in several reaction systems [24–29]. The significant increase in the photocatalytic activity with coupling rutile and anatase results from photo-induced interfacial electron transfer process. Within mixed-phase titania there is a morphology of nanoclusters containing atypically small rutile crystallites interwoven with anatase crystallites. The transition points between these two phases allowed for rapid electron transfer [24–26].

The nanometer size and high dispersion creates large surface area and quantum effect to promote photoactivity. Fig. 3 shows the

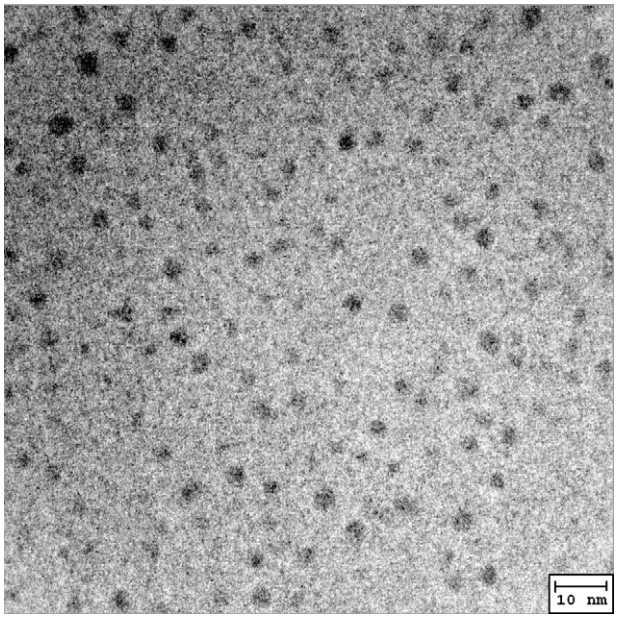

Fig. 3. TEM image of nano-TiO_2.

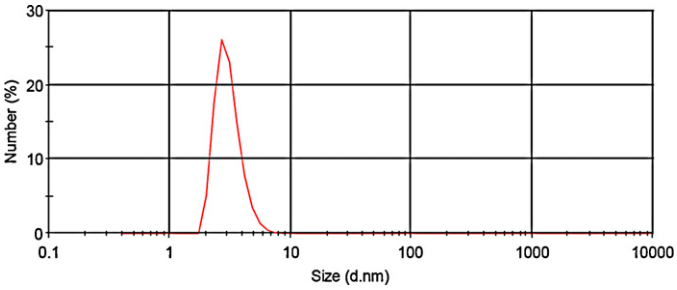

Fig. 4. Size statistics graph of nano-TiO_2 size distribution test.

Table 3
Characteristics of TiO_2 samples.

Characteristics	Nano-TiO_2	Degussa P25
Crystallite size (nm)	<10	30
BET surface area (m^2/g)	67	50
Band gap	3.14	3.14 [30]

TEM image of the nano-TiO_2. It shows the nano-TiO_2 powders are highly dispersed. Through special surface modification, the nano-TiO_2 can be highly dispersed in water without dispersing agents and/or ultrasonic stirring processes. Additionally, the aquatic suspension appeared clear and transparent. The nano-TiO_2 particles can be classified as nano-crystalline TiO_2 powders. The particle sizes are typically smaller than 10 nm (Figs. 2–4). The nano-TiO_2 powders are much smaller than typical commercial ones. The specific surface areas and other characteristics of the particle samples are shown in Table 3. The nano-TiO_2 exhibited higher BET surface area than the commercial P25. Our results show that the actual specific surface area of the well dispersed nano-TiO_2 in water is much higher than the result of the BET surface area test because of the nano-size effect. Fig. 5 presents that the band gap energy of the nano-TiO_2 is 3.14 eV. It is lower than pure anatase (3.2 eV) and equal to commercial P25.

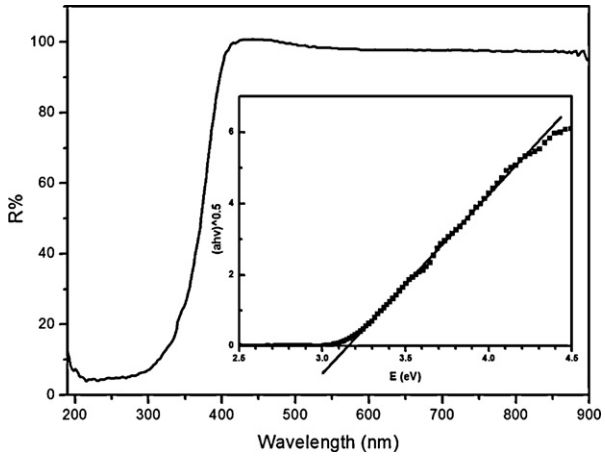

Fig. 5. Band gap energy of nano-TiO_2.

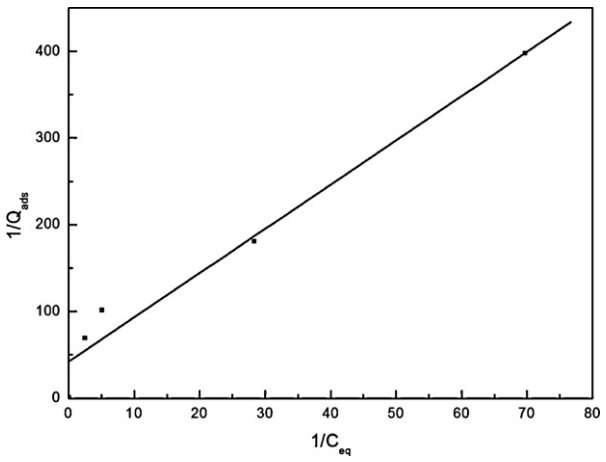

Fig. 6. Transformation of Langmuir isotherm: reciprocal of the quantity adsorbed as a function of the reciprocal of equilibrium concentration.

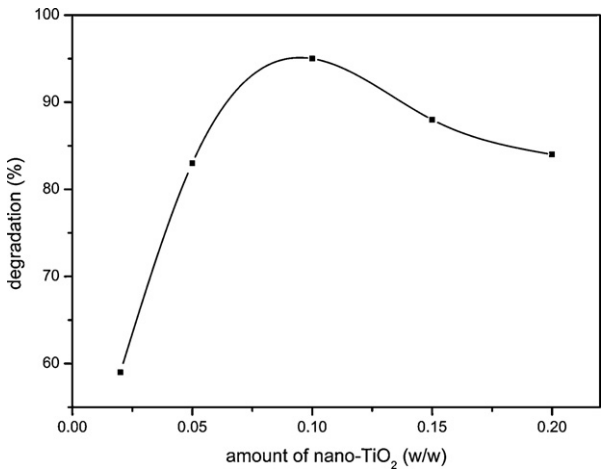

Fig. 7. Effect of amount of nano-TiO_2 on photodegradation of hexazinone. Volume = 10 ml; initial concentration of hexazinone = 5 mg/l; pH of the medium = 6.4; irradiation time = 30 min.

3.3. Adsorption on TiO_2 in the dark

The adsorption of the hexazinone on TiO_2 surface in the dark is important to the photocatalytic degradation process. A series of experiments were carried out in the dark to study the isotherm adsorption. The adsorption equilibrium was rapidly reached (in 20 min). As a consequence for the following experiments, the herbicide solutions were shaken in the dark for 30 min before being irradiated to ensure that adsorption equilibrium was reached.

It was observed that the adsorbed quantity (Q_{ads}) increased with equilibrium concentration (C_{eq}). This result agrees with the classical Langmuir adsorption model, followed by numerous compounds in aqueous suspension according to:

$$\theta = \frac{Q_{ads}}{Q_{max}} = \frac{K_{ads}C_{eq}}{1 + K_{ads}C_{eq}} \quad (1)$$

where θ is the TiO_2 surface coverage, Q_{ads} is the adsorbed quantity, Q_{max} is the maximal adsorbable quantity, C_{eq} is the concentration of the compound at the adsorption equilibrium and K_{ads} is the Langmuir adsorption constant (specific of the pair compound/catalyst).

The linear transformation of Eq. (1) can be expressed by the function $1/Q_{ads} = f(1/C_{eq})$:

$$\frac{1}{Q_{ads}} = \frac{1}{Q_{max}} + \frac{1}{Q_{max}K_{ads}C_{eq}} \quad (2)$$

In Fig. 6, the ordinate at the origin is equal to the reciprocal of Q_{max}, whereas K_{ads} can be calculated from the slope α ($=1/Q_{max}K_{ads}$). In Table 4, adsorption parameters for hexazinone are reported. In the adsorption experiment the pH of the aqueous suspensions was 6.5 and the amount of the TiO_2 was 0.1 wt%.

3.4. Photocatalytic degradation of hexazinone

For the subsequent experiments, the hexazinone solution was magnetically stirred in the dark for 30 min before irradiating the reactor to ensure that adsorption equilibrium. In the absence of TiO_2, no herbicide conversion was obtained indicating that the system was working in a pure photocatalytic regime. The photocatalytic degradation experiments were completed after the adsorption equilibrium was reached. Parametric effects and analyses were performed on amount of nano-TiO_2, pH and irradiation time.

Table 4
Adsorption characteristics of hexazinone: linear regression coefficient (r^2) of Langmuir linear expression, Langmuir constant (K_{ads}), Gibbs function (ΔG), maximal adsorbable quantity (Q_{max}), and maximal coverage of TiO_2 adsorption sites (θ_{max}).

Compound	r^2	K_{ads} (l/μmol)	$\Delta G = RT \ln K_{ads}$ (kJ/mol)	Q_{max} (μmol)	θ_{max} (%)
Hexazinone	0.99	5.79	−4.28	0.03	0.32

3.4.1. Effect of the amount of nano-TiO_2

Experiments were conducted to test the effect of the amount of catalyst for giving a concise operation condition. After adsorption in the dark, the samples containing various amounts of nano-TiO_2 were irradiated for 30 min. Fig. 7 shows that degradation increased from 85 to 95% when the amount of nano-TiO_2 increased from 0.02 to 0.1 wt%. However, degradation slightly decreased after the ratio of 0.1%. Thus, 0.1 wt% of nano-TiO_2 aquatic suspension was used and found to be adequate for photo-oxidation of 95% of 5 mg/l hexazinone in 30 min. Through repeated experiments, we have found that higher amounts (>0.1 wt%) of nano-TiO_2 showed slightly negative effect on the degradation. This can be explained in terms of availability of active sites on nano-TiO_2 surface and the light penetration of photo-activating light into the suspension. Excess of TiO_2 particles maybe become aggregated on the catalyst and some parts of the catalyst surface may therefore become unavailable for photocatalytic degradation.

3.4.2. Effect of Initial pH

Several tests were performed to observe the effect of pH on photocatalytic degradation. Fig. 8 shows the complete degradation of hexazinone was achievable under the neutral conditions. It is also shown that the degradation increases from 65% at pH 1.0 to 95% at pH 6.5, and then decreases to 55% at pH 10. This can be explained by both the surface chemical state of TiO_2 and the ionization state of ionizable organic molecules at different pH. The point of zero charge (pH_{PZC}) for the TiO_2 is about 6.8–7.2. When the TiO_2 suspension is acid or nearly neutral, the surface of TiO_2 is positively charged. When the reaction was conducted at nearly neutral condition (pH 6.5 in our study), TiO_2 solution becomes positively charged, and the hexazinone molecule will have a lone pair in the nitrogen atoms. Under this condition, hexazinone will be preferentially adsorbed on the TiO_2 surface due to electrostatic attraction and eventually leading to its complete degradation. However, when the pH of the TiO_2 solution is below or above the pH_{PZC}, TiO_2 and hexazinone will be both positively (or negatively) charged. Due to the electrostatic repulsion between the cations and TiO_2 particles, the hexazinone

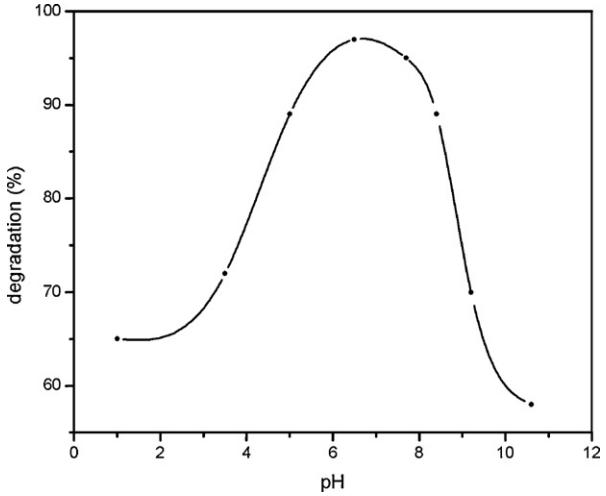

Fig. 8. Effect of initial pH on hexazinone photo-degradation.

solution will be poorly absorbed on the TiO_2 surface, which is considered an important step for photocatalysis [11,12,16].

3.4.3. Effect of irradiation time and degradation kinetics

Under optimized conditions (initial concentration of hexazinone = 5 mg/l; the amount of nano-TiO_2 = 0.1 wt%; pH of the medium = 6.5), the effect of irradiation time on hexazinone is shown in Fig. 9. It was observed that the degradation increased over the irradiation time, and the degradation was near complete within 40 min. In order to determine the kinetics of photo-degradation, the relationship between $\ln(C/C_0)$ and irradiation time was plotted (Fig. 10). It was found that the degradation reaction of hexazinone under the catalysis of the nano-TiO_2 basically obeyed to the first order reaction kinetics, according to the equation:

$$-\frac{dC}{dt} = k_{obs}C \tag{3}$$

where C is the herbicide concentration and k_{obs} is the observed first order rate constant. In this case, according to the Langmuir–Hinshelwood model, the Langmuir–Hinshelwood equation can be expressed as:

$$-\frac{dC}{dt} = r = k_{LH}\theta = \frac{k_{LH}K_{LH}C}{1 + K_{LH}C} \tag{4}$$

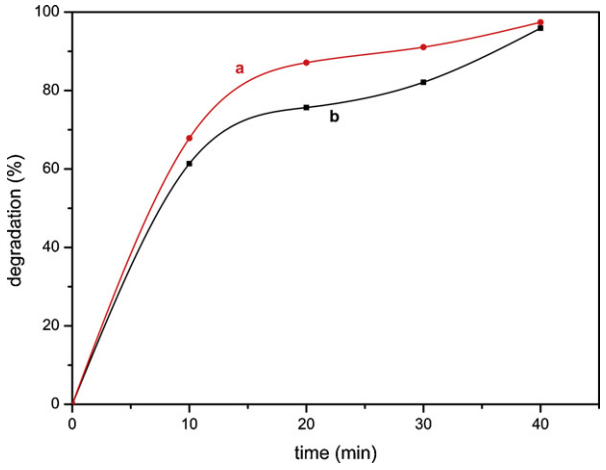

Fig. 9. Effect of irradiation time on photo-degradation of hexazinone (a) effect of nano-TiO_2 and (b) effect of Degussa P25.

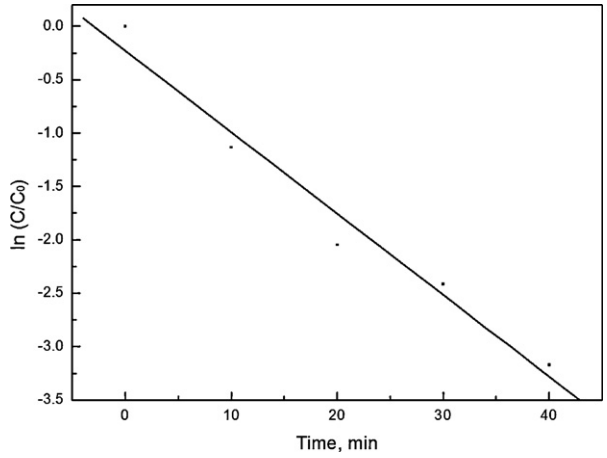

Fig. 10. The degradation kinetics of hexazinone by means of plotting $\ln(C/C_0)$ vs. time.

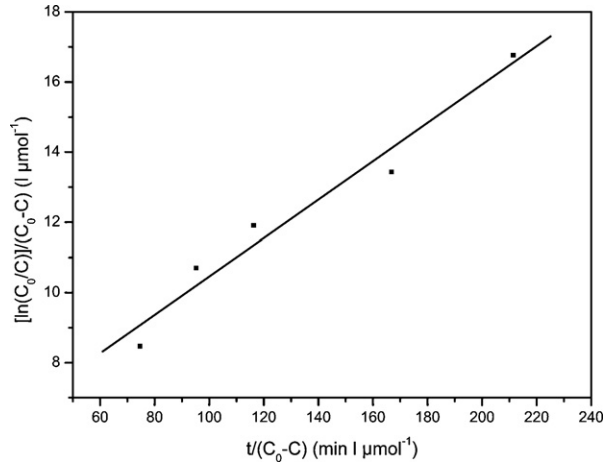

Fig. 11. Linearization of Langmuir–Hinshelwood isotherm.

where r is the reaction rate, k_{LH} is the true rate constant, K_{LH} is the Langmuir–Hinshelwood adsorption constant, C is the concentration of hexazinone. While $t = 0$, $C = C_0$, the integral of the Eq. (4) can be expressed by the linear form function $\frac{\ln(C_0/C)}{C_0/C} = f(t/(C_0 - C))$

$$\frac{\ln(C_0/C)}{C_0/C} = k_{LH}K_{LH}t\frac{1}{C_0 - C} - K_{LH} \tag{5}$$

The linear form of Langmuir–Hinshelwood model of hexazinone decomposition is presented in Fig. 11. The linear plots confirm the Langmuir–Hinshelwood relationship and indicate that adsorption represents the initial step in the photocatalytic process. The slope provides the K_{LH} value which is shown in Table 5. In the preceding section (see Table 4), the K_{ads} agrees well with K_{LH} value. This result indicates that K_{LH} reflects the adsorption affinity of hexazinone for the TiO_2 surface.

Table 5
Degradation kinetic parameters of hexazinone: linear regression coefficient (r^2) of Langmuir–Hinshelwood isotherm, the true rate constant (k_{LH}), the Langmuir–Hinshelwood adsorption constant (K_{LH}).

Compound	r^2	k_{LH} (µmol/(l min))	K_{LH} (l/µmol)
Hexazinone	0.98	0.01	5.04

3.5. Comparison of nano-TiO_2 with Degussa P25

Degradation effectiveness of nano-TiO_2 and Degussa P25 was compared under identical experimental conditions (volume = 25 ml; concentration of hexazinone = 5 mg/l; amount of each Degussa P25 and nano-TiO_2 = 0.1 wt%; pH 6.4). Fig. 9 shows that after 40 min irradiation, hexazinone molecules were completely decomposed by both Degussa P25 and the nano-TiO_2. Moreover, the nano-TiO_2 possessed better photocatalytic property as seen by the higher degradation percentage in the same irradiation time during the photocatalytic degradation. The observation was probably due to the higher utilization of photo-induced interfacial electrons and holes by the mixed-phase crystal microstructure and the well dispersed nano particles.

3.6. Identification of the photocatalytic by-products

Samples of the irradiated solutions were analyzed by LC–MS/MS in order to identify the photocatalytic by-products. The results are shown in Figs. 12 and 13. The structures of the principal compounds are identified by interpretation of their MS full scan and MS/MS daughter scan spectra data presenting their molecule ions and molecular ion fragments with respect to *m*/*z*.

Fig. 12a shows the LC–MS spectrum of the original hexazinone aqueous solution. As can be seen, one signal of molecule ion corresponds to positive ion at *m*/*z* 253 after trapping H^+ in the electrospray ionization process at atmospheric pressure. Fig. 12b shows the spectrum of hexazinone in TiO_2 suspension which was soaked for 30 min in the dark. The spectrum only shows the signal of the hexazinone molecule and trace amount of impurity in TiO_2 suspension without any information of the photocatalytic degradation by-products. This indicates that hexazinone molecules are only degradable under irradiation. Photocatalytic degradation by-products (*m*/*z* 267, 239, 102) were generated as shown in Fig. 12c. By-product 1 (*m*/*z* 267) and by-product 2 (*m*/*z* 239) were first identified by Reiser et al. [31]. Compared to the previous study, smaller molecule by-products were also identified such as by-product 6 (*m*/*z* 102). It is important to note that by-product 6 showed the highest intensity signal in Fig. 12c. Additionally, degradation by-products (*m*/*z* 241, 223, 147) were generated (Fig. 12d) with longer irradiation time. After 40 min of irradiation, only weak signals of by-product 6 and the nano-TiO_2 suspension (Fig. 12e) were observed. This indicated that the hexazinone molecules were decomposed by nano-TiO_2. The LC–MS/MS daughter scan spectra (Fig. 13) showed the molecular ion fragments of the by-products. Using the information, molecular structures can be identified and proposed.

A probable total degradation pathway of hexazinone is proposed for the first time. From the results, degradation of hexazinone may occur via the following proposed steps (see Fig. 14):

(i) primary by-product 1 is formed by the hydroxylation and ketonization of the hexatomic ring. During photocatalytic oxidation in water medium, $^{\bullet}OH$, H_2O_2 and $O_2^{\bullet-}$ reactive oxygen species are strongly electrophilic and oxidizing, and it is apt to attack the hexatomic ring leading to oxidation and further decomposition of the organic pollutant. Another primary product is by-product 2 formed by cleaving dimethylamine group to give methylamine group on the side chain of triazinone.
(ii) azomethine bond is covalently hydrated and ketonization, followed by eliminating dimethylamine or methylamine group to form by-product 3 or by-product 4.
(iii) by-product 5 is identified for the first time in the degradation study of hexazinone. It is formed by cleaving the hexatomic ring on the side chain of triazinone. This is a new finding

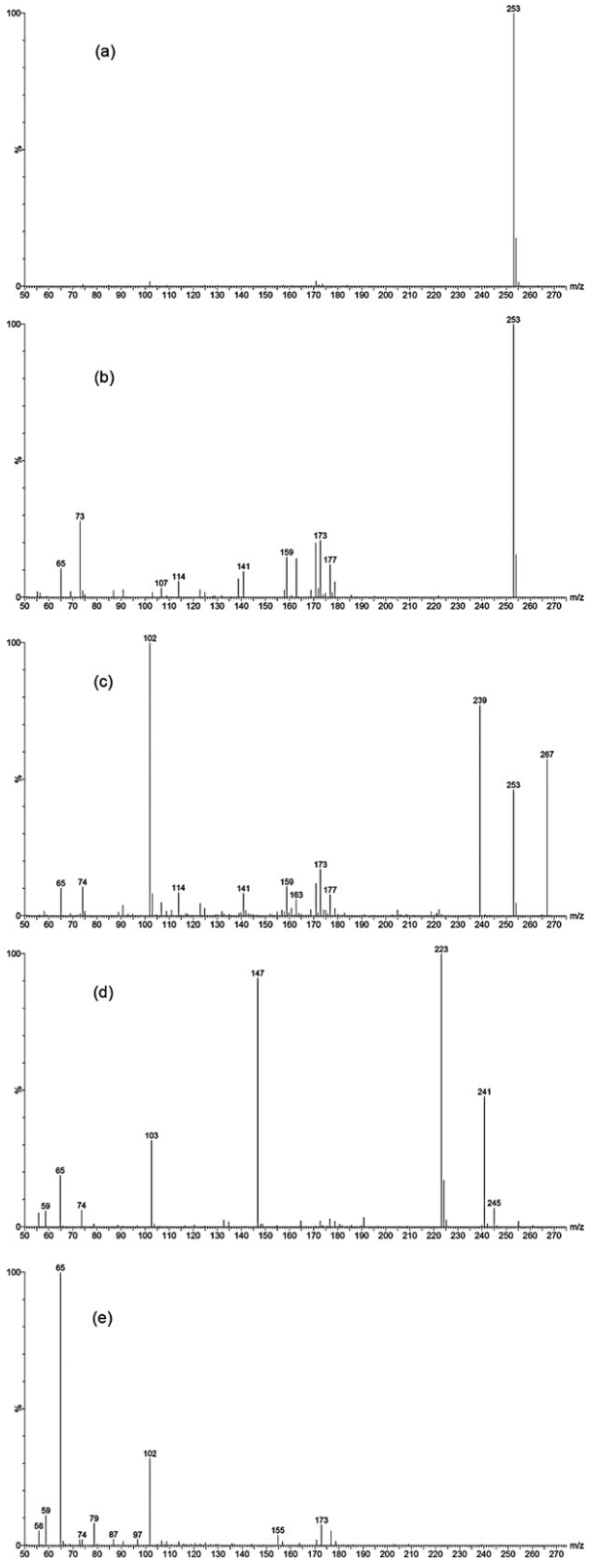

Fig. 12. LC–MS spectra of (a) the original hexazinone aqueous solution (b) hexazinone in TiO_2 suspension after soaked in the dark (c) hexazinone in TiO_2 suspension after irradiation 20 min (d) hexazinone in TiO_2 suspension after irradiation 30 min (e) hexazinone in TiO_2 suspension after irradiation 40 min.

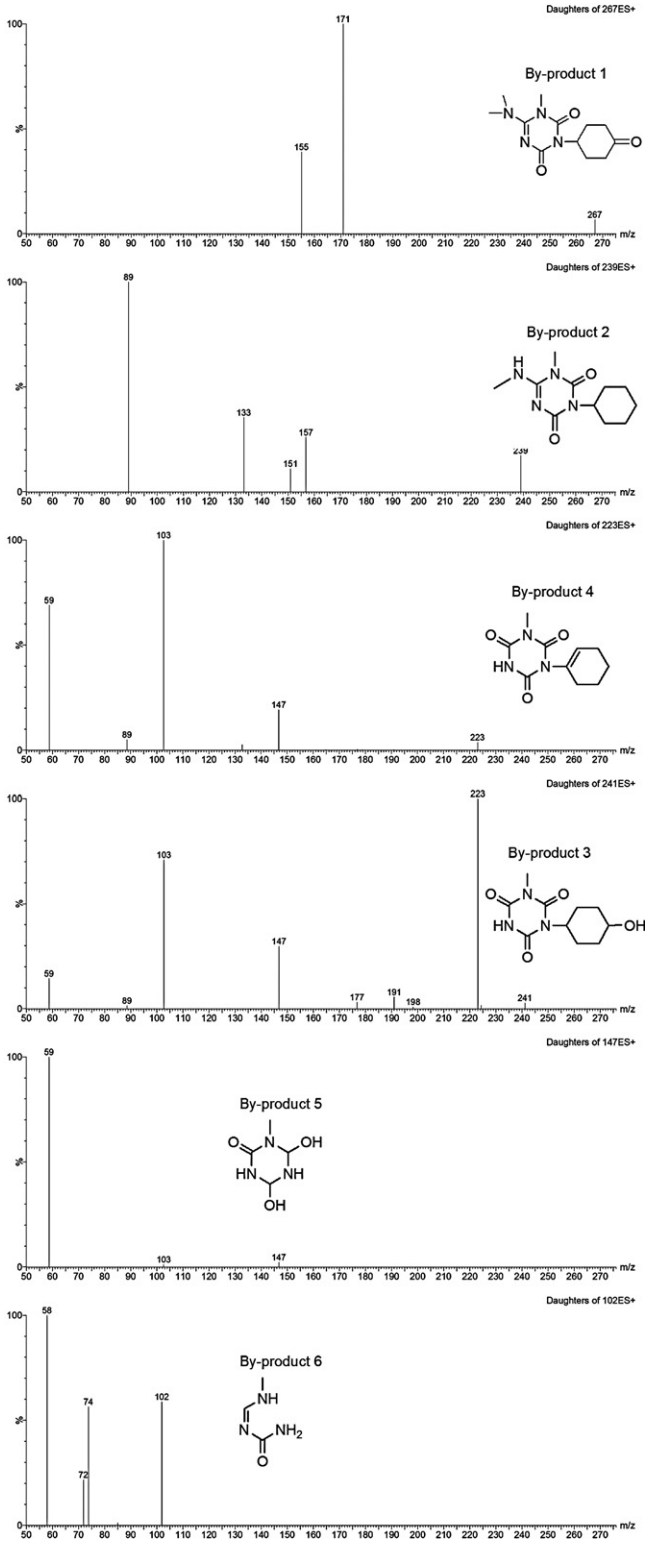

Fig. 13. LC–MS/MS spectra of the photocatalytic degradation by-products of hexazinone.

because it is a smaller molecular by-product compared to previous reports.

(iv) by-product 6 is also identified for the first time. It is formed by cleaving the triazine ring and further dehydration process. The formation of by-product 6 further enhances full degradation of hexazinone. Further oxidation to permineralization may occur

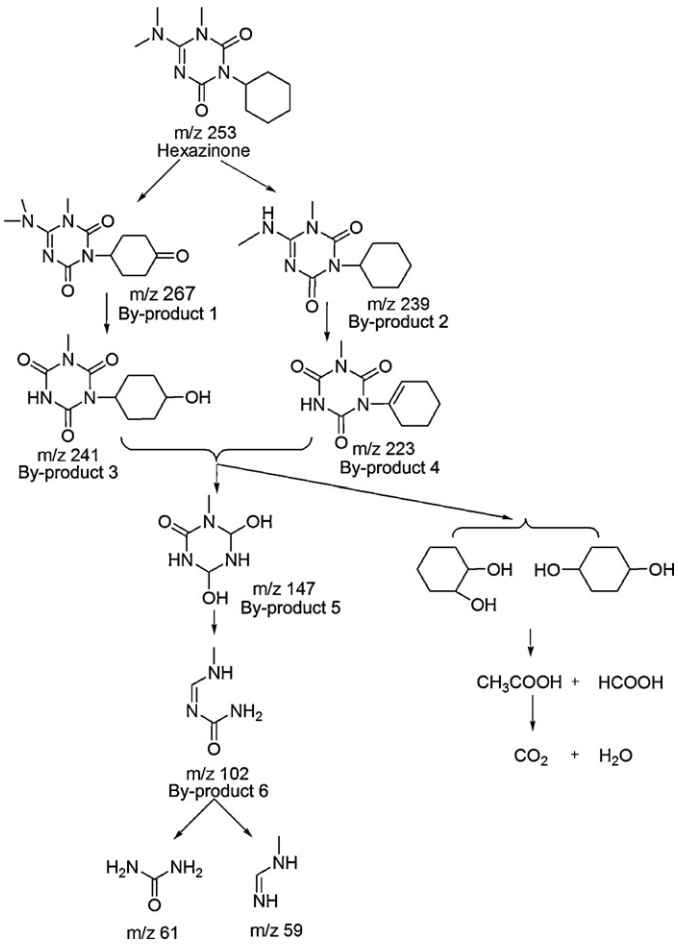

Fig. 14. Probable photocatalytic degradation pathway of hexazinone.

to give the final products, such as urea, carbon dioxide and water.

4. Conclusions

The present work investigates the photocatalytic degradation of hexazinone using mixed-phase crystalline nano-TiO_2 aqueous suspender under UV irradiation. Influences of various parameters, such as adsorption, concentration of nano-TiO_2, pH and irradiation time on the photocatalytic process are performed. Complete degradation is achieved within 40 min of irradiation. The proposed nano-TiO_2 solution has better photocatalytic degradation performance under the same irradiation time when compares to Degussa P25. The proposed photocatalytic degradation process fits the Langmuir–Hinshelwood model. Furthermore, the degradation by-products are identified by LC–MS/MS technique. A probable pathway for the formation of photocatalytic degradation by-products is proposed. The degradation process is complete and the final products are nontoxic water, carbon dioxide and urea. To support the study of the photocatalysis degradation, a rapid, sensitive, highly confirmed and highly specified UPLC–MS/MS method under MRM mode for the determination of hexazinone in water is developed. The results show that the LOD is 0.05 μg/l and the LOQ is 0.16 μg/l. The photocatalytic degradation and the determination methodology show great promise for routine remediation and monitoring of dissolved pollutants in water. The potential for a wide range of practical applications is expected.

Acknowledgements

The authors would like to acknowledge financial support for this work provided by the Chinese Universities Scientific Fund (ZD0904) and the Beijing Education Commission Joint Project Fund (2011).

References

[1] H.G. Peterson, C. Boutin, K.E. Freemark, P.A. Martin, Toxicity of hexazinone and diquat to green algae diatoms, cyanobacteria and duckweed, J. Aquat. Toxicol. 39 (1997) 111–134.
[2] USA Environmental Protection Agency, Registration Eligibility Decision (RED) Hexazinone, EPA 738-R-94-022, September 1994, p. 121.
[3] R.N. Wilkins, G.T. Tanner, R. Mulholland, D.G. Neary, Use of hexazinone for understory restoration of a successionally-advanced xeric sandhill in Florida, J. Ecol. Eng. 2 (1993) 31–48.
[4] D.T. Kubilius, R.J. Bushway, Determination of hexazinone and its metabolites in groundwater by capillary electrophoresis, J. Chromatogr. A 793 (1998) 349–355.
[5] D.C. Bouchard, T.L. Lavy, High-performance liquid chromatographic determination of hexazinone residues in soil and water, J. Chromatogr. 270 (1983) 396–401.
[6] J.B. Fischer, J.L. Michael, Thermospray ionization liquid chromatography-mass spectrometry and chemical ionization gas chromatography mass spectrometry of hexazinone metabolites in soil and vegetation extracts, J. Chromatogr. A 704 (1995) 131–139.
[7] Y. Zhu, Q. Li, Movement of bromacil and hexazinone in soils of Hawaiian pineapple fields, J. Chemosphere 49 (2002) 669–674.
[8] D. Neary, P. Bush, J. Douglass, Off-site movement of hexazinone in stormflow and baseflow from forest watersheds, J. Weed Sci. 31 (1983) 543–547.
[9] H.L. Wang, S.X. Xu, C.X. Tan, X.D. Wang, Anaerobic biodegradation of hexazinone in four sediments, J. Hazard. Mater. 164 (2009) 806–811.
[10] M. Privman, P. Zuman, The role of protonation hydration, elimination, and ring opening in the electroreduction of hexazinone, J. Electroanal. Chem. 455 (1998) 235–246.
[11] L. Gu, Z.X. Chen, C. Sun, B. Wei, X. Yu, Photocatalytic degradation of 2, 4-dichlorophenol using granular activated carbon supported TiO_2, J. Desalinatn. 263 (2010) 107–112.
[12] E. Vulliet, J.M. Chovelon, C. Guillard, J.M. Herrmann, Factors influencing the photocatalytic degradation of sulfonylurea herbicides by TiO_2 aqueous suspension, J. Photochem. Photobiol. A: Chem. 159 (2003) 71–79.
[13] F. Fresno, C. Guillard, J.M. Coronado, J.M. Chovelon, D. Tudela, J. Soria, J.M. Herrmann, Photocatalytic degradation of a sulfonylurea herbicide over pure and tin-doped TiO_2 photocatalysts, J. Photochem. Photobiol. A: Chem. 173 (2005) 13–20.
[14] C.L. Bahena, S.S. Martínez, D.M. Guzmán, M.T. Hernández, Sonophotocatalytic degradation of alazine and gesaprim commercial herbicides in TiO_2 slurry, J. Chemosphere 71 (2008) 982–989.
[15] S. Erdemoğlu, S.K. Aksu, F. Sayılkan, B. İzgi, M. Asiltürk, H. Sayılkan, F. Frimmel, Ş. Gücer, Photocatalytic degradation of Congo Red by hydrothermally synthesized nanocrystalline TiO_2 and identification of degradation products by LC–MS, J. Hazard. Mater. 155 (2008) 469–476.
[16] S. Chusaksri, J. Lomda, T. Saleepochn, P. Sutthivaiyakit, Photocatalytic degradation of 3,4-dichlorophenylurea in aqueous gold nanoparticles-modified titanium dioxide suspension under simulated solarlight, J. Hazard. Mater. 190 (2011) 930–937.
[17] B. Zielińska, J. Grzechulska, B. Grzmil, A.W. Morawski, Appl. Catal. B 35 (2001) 1–7.
[18] G. Sivalingam, K. Nagaveni, M.S. Hegde, G. Madras, Appl. Catal. B 45 (2003) 23–38.
[19] R.A. Spurr, H. Myers, Quantitative analysis of anatase–rutile mixtures with an X-ray diffractometer, Anal. Chem. 29 (1957) 760–762.
[20] K. Prasad, D.V. Pinjari, A.B. Pandit, S.T. Mhaske, Phase transformation of nanostructured titanium dioxide from anatase-to-rutile via combined ultrasound assisted sol–gel technique, Ultrason. Sonochem. 17 (2010) 409–415.
[21] M. Mei, Z.X. Du, Y. Chen, QuEChERS-ultra-performance liquid chromatography tandem mass spectrometry for determination of five currently used herbicides, J. Chin. J. Anal. Chem. 39 (2011) 1659–1664.
[22] H. Tada, M. Tanaka, Dependence of TiO_2 photocatalytic activity upon its film thickness, Langmuir 13 (1997) 360–364.
[23] Z. Ding, G.Q. Lu, P.F. Greenfield, Role of the crystallite phase of TiO_2 in heterogeneous photocatalysis for phenol oxidation in water, J. Phys. Chem. B 104 (2000) 4815–4820.
[24] T. Kawahara, T. Ozawa, M. Iwasaki, H. Tada, S. Ito, Photocatalytic activity of rutile–anatase coupled TiO_2 particles prepared by a dissolution–reprecipitation method, J. Colloid Interface Sci. 267 (2003) 377–381.
[25] S. Bakardjieva, J. Šubrt, V. Štengl, M.J. Dianez, M.J. Sayagues, Photoactivity of anatase–rutile TiO_2 nanocrystalline mixtures obtained by heat treatment of homogeneously precipitated anatase, J. Appl. Catal. B 58 (2005) 193–202.
[26] T. Ohno, K. Tokieda, S. Higashida, M. Matsumura, Synergism between rutile and anatase TiO_2 particles in photocatalytic oxidation of naphthalene, J. Appl. Catal. A 244 (2003) 383–391.
[27] T. van der Meulen, A. Mattson, L. Österlund, A comparative study of the photocatalytic oxidation of propane on anatase, rutile, and mixed-phase anatase–rutile TiO_2 nanoparticles: Role of surface intermediates, J. Catal. 251 (2007) 131–144.
[28] M. Kanna, S. Wongnawa, Mixed amorphous and nanocrystalline TiO_2 powders prepared by sol–gel method: characterization and photocatalytic study, J. Mater. Chem. Phys. 110 (2008) 166–175.
[29] R.I. Bickley, T.G. Carreno, J.S. Lees, L. Palmisano, R.J.D. Tilley, A structural investigation of titanium dioxide photocatalysts, J. Solid State Chem. 92 (1991) 178–190.
[30] B. Zielińska, J. Grzechulska, B. Grzmil, A.W. Morawski, The pH influence on photocatalytic decomposition of organic dyes over A11 and P25 titanium dioxide, J. Appl. Catal. B 45 (2003) 293–300.
[31] R. Reiser, I. Belasco, R. Rhodes, Identification of metabolites of hexazinone by mass spectrometry, J. Biomed. Mass Spectrom. 10 (1983) 581–585.